Multi-scale simulation of the atomization of a liquid jet in cross-flow in the presence of an acoustic perturbation

D. Zuzio[1]*, S. Thuillet[1], O. Rouzaud[1], J.-M. Senoner[1], C. Laurent[1], P. Gajan[1]

[1]Multi-Physics Department for Energetics, ONERA/DMPE - Université de Toulouse, F-31055, Toulouse, France

*Corresponding author: davide.zuzio@onera.fr

Abstract

The reduction of pollutant emissions is currently a major concern in the aerospace sector. Among the proposed solutions, lean combustion appears as an effective technology to reduce the environmental impact. However, this type of technology may also favour the appearance of combustion instabilities. These instabilities, resulting from a thermo-acoustic coupling, can lead to irreversible damage to the combustion chambers.

Experimental studies previously conducted at ONERA on a multipoint injector by Apeloig [1] highlighted the importance of atomization on the instabilities loop. Indeed, the fuel vapour concentration near the injection zone has been shown to fluctuate in accordance with the imposed acoustic perturbation. The driving mechanism would then result from a flapping motion of the liquid jets in the multiple injection points, induced by the gas flow oscillations. This would in turn affect the characteristic convective timescales of the fuel, in the form of a spray or even of thin liquid films on the duct walls.

In order to characterize this interaction, this work focuses on the unsteady simulation of a round liquid jet in the presence of a transverse gas flow in a rectangular section duct. Following an experimental study (Bodoc [4]), the multi-scale numerical approach for multi-phase flows (Blanchard [3]), implemented in the ONERA CEDRE code, has been tested in presence of an imposed acoustic perturbation. This approach consists of the coupling of three models: a multi-fluid model able to capture the largest scales of the liquid column atomization; a dispersed phase approach for the atomized spray, and a “Shallow Water” approach for wall films. The coupling of these approaches is provided by dedicated atomization and impact models, which ensure liquid transfer between the three models.

Simulation results (Thuillet [14]) show that the multi-fluid solver is able to correctly capture the largest scales of the liquid jet. The simulated liquid jet trajectories match the experimental ones, as well as their dynamic response to the imposed acoustic perturbation. As the liquid is transferred to the dispersed phase solver, the jet motion deeply affects the spray formation and behaviour. Good agreement was found on the particle resulting mean velocity, but only partial agreement on the phase delay. An important wall deposition has been detected for particular jet positions as well.

Keywords

Liquid jet in crossflow, Multi scale, Multi phase, Acoustic perturbation

Nomenclature

Liquid Jet In Cross-Flow	=	LJICF	
Gas mean velocity at the jet location	=	U_0	[$m.s^{-1}$]
Liquid mean velocity at the jet location	=	U_j	[$m.s^{-1}$]
Jet diameter	=	d_j	[m]
Duct length from jet to outlet	=	L_c	[m]
Duct width from jet to outlet	=	W_c	[m]
Surface tension coefficient	=	σ	[$N.m^{-1}$]
Gas and liquid densities	=	ρ_g, ρ_l	[$kg.m^{-3}$]
Gas and liquid viscosities	=	μ_g, μ_l	[$Pa.s$]
Liquid volume fraction	=	α_L	[-]
Cross-flow Weber number	=	$We_j = \rho_g (U_0)^2 d_j / \sigma$	[-]
Cross-flow Reynolds number	=	$Re_j = \rho_g U_0 d_j / \mu_g$	[-]
Momentum flux ratio	=	$q = \rho_l U_j^2 / \rho_g U_0^2$	[-]

Introduction

Aeronautical multi-point injectors have been developed to better control the air and fuel mixing, in a regime of lean premixed combustion. They are based on a double fuel circuit. A first central pressure injector is devoted to flame stabilization, while the high flow is supplied by multiple circular injection holes surrounding the pressure injector. As these injection holes are oriented perpendicularly to the gaseous flow field, they result in a so called “Liquid Jet In Cross Flow” (LJICF) configuration. However, lean combustors are more prone to the development of thermos-acoustic/ combustion instabilities, resulting from an unstable coupling between the unsteady heat release due to combustion and acoustic pressure oscillations travelling within the combustion chamber (see for example Bauerheim [2], Candel [5], Ducruix [7], Nicoud [10], Poinsot [11]). These instabilities can lead to excessive engine vibration and possible irreversible damage of the propulsion system.

ONERA performed an experimental study of a multi-point injector (Apeloig [1]) with the thermo-acoustic rig (LOTAR). A siren was used to force the rig acoustics at different frequencies. The purpose of this study was to better understand the behaviour of the jet atomization in presence of combustion instabilities. Indeed, PLIF (Particle Laser Induced Fluorescence) visualizations have shown a variation of the liquid kerosene spatial distribution during an instability cycle. The cyclic change in local fuel density has been explained by the unsteady behaviour of the cross-flow atomizing the liquid jets in the multipoint zone: a variation of gas velocity, or liquid-gas momentum flux ratio, may strongly affect the jet trajectory. Moreover, an important part of the liquid mass flow can in consequence directly impact the walls, forming a film which significantly changes the characteristic convection time of the liquid.

In order to obtain a better understanding of the interaction between atomization and acoustic perturbations, a simplified test rig (SIGMA) has been built at ONERA (Bodoc [4]), focusing on a single injection point in the form of a water jet in gaseous cross-flow inside a confined duct. The experiences are devoted to study the effect of imposed acoustic perturbations on the atomization of the jet, and the subsequent characteristics of the spray exiting the duct.

The aim of this paper is to assess the ONERA CEDRE multi-solver methodology for the simulation of the LJICF atomization in the SIGMA experience (Thuillet [14]). This numerical approach should address the following points:

- Simulation of the main liquid body behaviour.
- Atomization modelling and generation of the cloud of droplets.
- Droplet impinging on solid walls and formation of a thin film.
- Simulation of an unsteady regime, i.e. under an imposed acoustic perturbation.

Three numerical models interact to achieve these objectives. A multi-fluid model captures the larger scales of the liquid jet breakup, mainly the jet bending and deformation under the shearing effect of the gas: the trajectory of the liquid, strongly depending on the momentum flux ratio q, should be correctly reproduced, while it would not be the case if droplets were directly injected in the duct. Surface tension effects are taken into account and contribute to the coherence of the column. As atomization occurs, the smaller length scales became quickly under-resolved, and the interface starts to diffuse. Physically, ligaments and liquid blobs (smaller than typical LES mesh sizes) are formed and separate from the main body of the jet, undergoing then secondary atomization which leads to the formation of the droplets. The atomization model from Blanchard [2] allows the coupling with a dispersed phase solver, working as an advanced numerical injector. The droplets are dynamically generated ensuring local mass, momentum and energy conservation. The spray evolution is described by a well established dispersed phase model, resolved in a Lagrangian framework (an Eulerian framework is available as well, as in Gaillard [8]). As the droplets impact the duct walls, a Shallow-Water model (Laurent [9]) allows the tracking of a thin film generated by droplet impingment. Any unsteady effect on the two-phase solution should therefore affect its characteristics like its thickness and velocity. The simulation results were compared to the experimental measurements done on the SIGMA test rig.

Reference test rig

ONERA carried out an experimental investigation (Bodoc [4]) of a LJICF in a duct flow, under an imposed acoustic perturbation. The purpose of this study was to better understand the behaviour of the jet atomization in presence of combustion instabilities, as well as the formation of liquid films when the droplets impact the duct walls.

The experimental configuration consists of a duct with a rectangular cross-section, where the liquid is injected through a circular orifice located on the bottom wall, as depicted in **Figure 1**. A ramp reduces the duct cross-section in order to stabilize the flow before the jet and minimize the gas turbulence intensity.

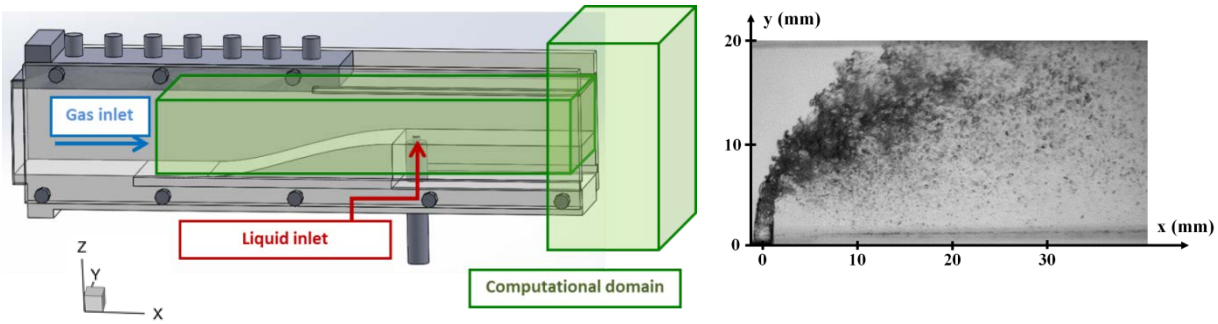

(a) Test rig *(b) Jet visualization*

Figure 1. Experimental SIGMA test rig and corresponding simulation numerical domain; an experiment visualization.

The test rig dimensions are detailed in Table 1, while the relevant quantities of the reference operating point are given in Table 2 (a sketch of the numerical simulation domain is highlighted in Figure 1(a) as well). Figure 1(b) shows an instantaneous visualization of the jet atomization. The high Weber number is typical of a *shear breakup* regime (Sallam [13], Wu [15]). In this regime the shearing effect is sufficiently strong to generate a very fine droplet cloud in a short distance in reason of a stripping mechanism working together with the breakup of the main column (*column breakup*). Upstream, a pneumatic loudspeaker delivers a periodic one-dimensional acoustic perturbation, in the form of a steady planar (yz-normal) sinusoidal acoustic wave of controlled amplitude and phase. The frequency of $f = 177\ Hz$ was chosen in order to set a velocity node on the location of the jet, thus providing the maximum effect on the liquid injection.

Square duct section	-	5 × 5	[*cm*]
Rectangular duct section	-	5 ×2	[*cm*]
Rectangular duct length	L_c	10	[*cm*]
Jet diameter	d_j	0.2	[*cm*]

Table 1. SIGMA dimensions.

Gas average velocity[1]	U_0	65	$[m.s^{-1}]$
Liquid mean velocity	U_j	6.3	$[m.s^{-1}]$
Momentum flux ratio	q	7.6	[-]
Cross-flow Weber	We_c	144	[-]
Cross-flow Reynolds	Re_c	8 847	[-]

Table 2. SIGMA nominal operating point.

The amplitude was chosen in order to ensure the onset of the jet flapping motion. The characteristics of the perturbed LJICF are presented in Table 3.

Gas average velocity	U_0	$57 \div 74$	$[m.s^{-1}]$
Momentum flux ratio	q	$6 \div 10.5$	[-]
Cross-flow Weber number	We_c	$105 \div 183$	[-]

Frequency	f	177	[Hz]
Amplitude	A_0	9.5	[%]

Table 3. Parameter variation range for the simulation with acoustic perturbation: velocity and non dimensional numbers.

Numerical strategy

CEDRE code

The ONERA CEDRE in-house platform ([6]) has been developed as a multi-physics software, able to deal with complex mono- and multi-phase flows. Within this work, three CEDRE modules will be used to efficiently perform an unsteady large scale simulation of the LJICF:

- CHARME: multi-fluid compressible Navier-Stokes solver;
- SPARTE: Lagrangian dispersed phase solver;
- FILM: Shallow Water solver for liquid films.

The CHARME solver is dedicated to the resolution of the gas and liquid phases where they are clearly distinguished. The two-phase aspect of the flow is taken into account by a multi-fluid solver, meaning that a set of conservation equations is solved for each phase. A mixture equation is solved for both momentum and energy, in a so-called four-equation model. The interface is implicitly captured by a diffuse interface model, taking into account surface tension effects.

[1] At the jet location.

The SPARTE solver is dedicated to the simulation of dilute dispersed-phase flows using a Lagrangian approach. It gives a mesoscopic (statistical) description of a cloud of particles, provided by the Williams-Boltzmann kinetic equation. The particles are assumed to be spherical and fully characterized by a set of variables including position, radius, velocity and temperature. Each particle carries the information of a set number of physical particles, this number being refereed to as "numerical weight".

The FILM solver is dedicated to the resolution of the Shallow Water equations, which model a liquid film on a solid wall under the assumption that the film height is small compared to the surface characteristic length.

Figure 2 shows a sketch of the proposed large scale simulation of the SIGMA LJICF as well as a simulation snapshot. Details about the solver interaction are provided in the subsequent section.

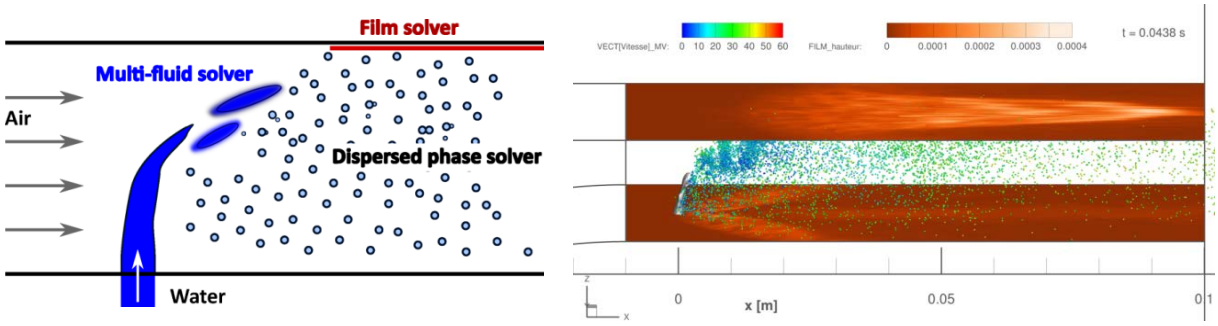

Figure 2. CEDRE multi-scale approach for the LJICF simulation. Multi-fluid resolution of the main liquid body, generation of a dispersed phase and wall deposition.

Multi-solver coupling terms

The multi-solver strategy involves the interaction of the three solvers, CHARME, SPARTE and FILM, in order to capture the different physical scales of the LJICF atomization. Two "layers" of interactions can be defined: the first is the classical exchange of information between the systems, while the second consists in an active dynamic transfer of liquid mass from one solver to another. This paragraph describes this second layer of exchanges.

- CHARME → SPARTE

This coupling is loosely called "atomization model" as it aims to simulate the pulverization of the liquid without an interfacial-refined simulation (see Blanchard [3]). The coupling consists in a transfer of liquid mass from the multi-fluid to the dispersed phase solver, and is meant to provide a high quality droplet injection, obtained by the time-resolved simulation of the largest-scale instabilities of the liquid core. A new Eulerian set of equations allows the interaction between the continuous form of the CHARME equations and the discrete form of the SPARTE parcels. It is activated whenever an under-resolution of the captured interface is detected, and acts as a local particle numerical injector: new particles are therefore dynamically generated in the computational domain. However, droplet diameter is at the moment a fixed model parameter.

- SPARTE → FILM

This coupling is devoted to the interaction between a surface and liquid droplets. The disperse phase solver SPARTE computes the source terms for modelling the film formation by spray impingement: the liquid mass is injected into the film model and the corresponding parcels removed from the dispersed phase solver. The hypothesis of full liquid deposition has been made within this study.

Results and discussion

Numerical set-up

A simulation of the SIGMA configuration has been performed (Thuillet [14]), in order to assess the capability of the large-scale multi-solver CEDRE approach. The spatial directions have been kept according to **Figure 1(a)**; the origin of the axes has been set on the jet location. The *x* measurements are therefore taken from the jet location. The domain corresponds loosely to the highlighted region in **Figure 1(a)**. The mesh is a structured Cartesian one for the sake of simplicity and accuracy; a local refinement has been imposed on the jet location, with a mesh size of about *80 µm* (~25 cells in the jet diameter). An implicit time discretization has been chosen, with a time step of $\Delta t = 1 \times 10^{-7}$ *s*. An effective parallelization on 128 processors enables to get a steady regime in approximately 10 hours CPU time, for an effective simulation time of *2.5 ms* per run. Based on the average droplet diameter measured by Bodoc et al. [4], the droplet diameter has been fixed at d_d = 40 *µm.* Gas and liquid inlet conditions are set to match the experimental values on the particular operating point depicted in **Table 2**. Inlet gas profiles were provided by a dedicated RANS simulation of the full *2 m* long duct and successfully validated against hot-

wire measurements. The liquid inlet condition is a flat profile set before the pipe section change. Free-flow conditions are imposed at the outflow location. Non-reflection conditions are imposed on the inlets and outlet.

Figure 2 presents a visualization of the three solvers interacting in the simulation of the jet inside the rectangular duct. At the *x = 0* location, the jet enters the channel. The *0.5* iso-contour of CHARME liquid phase (α_L) is shown to illustrate the simulation of the jet column body. As the values of α_L and its gradient drop under fixed thresholds, the atomization model locally injects numerical particles ("parcels"). The numerical particles are dynamically generated in cells where the multi-fluid liquid volume fraction and its gradient fall under prescribed thresholds. The values of these thresholds are respectively $\alpha_{thr} = 0.01$ and $\|\nabla\alpha\|_{thr} = 0.5$, these values being a reasonable compromise between the accuracy of the multi-fluid solution and the hypothesis of dispersed phase (the parcel volume is considered as negligible), see Blanchard [3] for more details. A fixed numerical weight has been set to $w_p = 10$, meaning that each parcel carries the information of ten physical droplets. The resulting total number of parcels is of the order of several millions, thus giving a good discretization of the spray. As the particles are generated, their velocity is initialized to the local cell mixture velocity[2]. The particles impacting the upper wall are removed, their mass and momentum added to the wall film. The film thickness is determined by the wall impingement rate; once formed up, the film advances with its own convective velocity.

Acoustic field

Figure 3 presents the pressure and gas velocity temporal signals obtained by a gas-only simulation of the acoustic wave propagation. A very good agreement was found with the measured fields, ensuring that the numerical jet sees the same fluctuating gaseous flow as the SIGMA jet. As the duct section is reduced by the ramp, the fluctuating component of the velocity increases, while the phase delay decreases. A plateau is attained by the phase delay in the constant section of the duct, after the jet location ($x/L_C = 0$). The acoustic perturbation induces a variation of the dimensional and non dimensional characteristics of the flow, as recalled in **Table 3**: these variations, in particular the *q* parameter variation, determine the unsteady jet, spray and film behaviours described in the following sections.

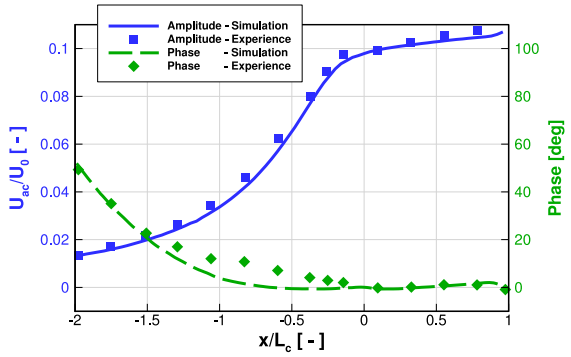

Figure 3. Velocity acoustic field in the duct, amplitude and phase delay. The jet is located at $x/L_C = 0$. Comparison with experience.

Jet behaviour

The variation of the momentum flux ratio *q* is expected to induce a notable trajectory variation around the unperturbed shape, and a consequent variation of the droplet concentration. The variation of the Weber number may have an impact on the droplet diameter; however no dynamic modelling has been introduced in the simulation. The film should also react to an unsteady impingement rate.

Figure 4 shows six instantaneous two-phase fields in an oscillation period at fixed phases Φ = *(0°,60°,120°,180°,240°,300°),* the reference phase being the sinusoidal signal of gas velocity at the jet location:

[0° - 60°] The beginning of a cycle corresponds to the instantaneous perturbation velocity on the jet equal to zero. The jet shape and trajectory as well as the velocity magnitude field are similar to the non perturbed case. The droplets near the jet are notably slower than those approaching the exit, which were affected by the previous fluctuation cycle.

[120° - 180°] The velocity signal reaches the highest values. The jet trajectory is the flattest. High velocity particles fill the duct, thus increasing the mass flow ratio at the exit of the duct. The upper wall impact location is shifted downstream.

[240° - 300°] The velocity signal reaches the lowest values. The ratio *q* is the lowest, so that the liquid jet

[2] The initial velocity of the particles still remains an open modelling question.

reaches its straightest position, almost vertical. Droplets with low initial velocity start to accumulate around the jet, and are very slightly accelerated downstream. The impinging rate on the upper wall is more important and the impact point shifts upstream, nearer to the jet location.

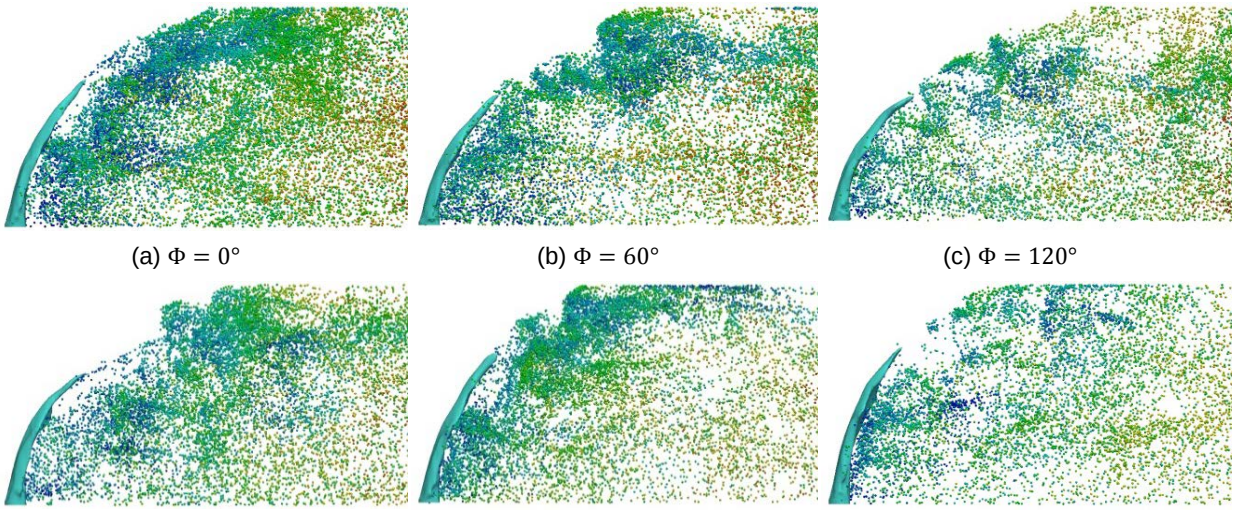

(a) $\Phi = 0°$ (b) $\Phi = 60°$ (c) $\Phi = 120°$

(d) $\Phi = 180°$ (e) $\Phi = 240°$ (f) $\Phi = 300°$

Figure 4. Instantaneous results of the LJICF under imposed acoustic perturbation, one full period. In white is the liquid jet α_L = 0.5, the scatter plot represents the particles, coloured by their absolute velocity.

Figure 5 shows the maximal and minimal trajectories of the jet (respectively at *130°* and *310°*) from both the experience and the simulation. The analysis of the instantaneous liquid column height (measured at a fixed x/L_C = *2.8)* in Figure 6 shows an excellent agreement in the jet dynamics as well, successfully comparing to the experimental signal in function of the phase.

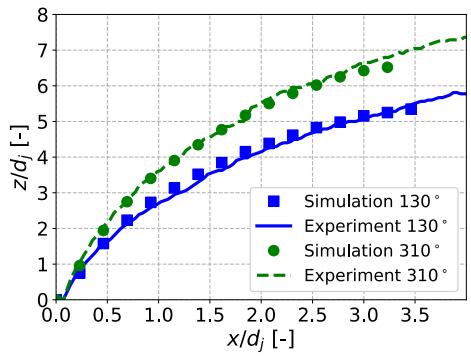

Figure 5. Maximal and minimal trajectories of the jet, at respectively $\Phi = (130°, 310°)$.

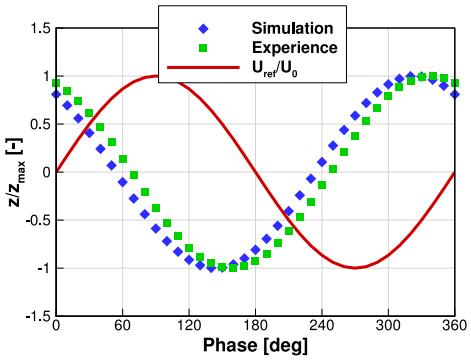

Figure 6. Jet column height in function of the phase, measured at a fixed point x/L_C = *2.8*.

Spray behaviour

The numerical spray was compared to the corresponding class of droplets from the experience. The average longitudinal velocity of the droplet was measured in the whole duct section and in a restricted section centred on the duct centreline[3], Figure 7(a). An excellent agreement was found in the second half of the duct, $x/L_C > 0.4$ while important differences appear near the jet location. The atomization model simplification hypothesis may have here negatively affected the droplets behaviour, and its effect should be further investigated. Figure 7(b) presents the droplet velocity amplitude and phase delay near the duct exit ($x/L_C = 0.8$). The experimental and the numerical data are in very good agreement: the spray average velocity near the outlet is significantly affected by the acoustic perturbation, thus the global liquid concentration at the exit of the test rig. This result seems to confirm the hypothesis done in Apeloig at al. [1], in which the fluctuations of kerosene vapour concentration in a multipoint injector would result from the flapping motion of the liquid clearing the multipoint injection points.

[3] Where the experimental punctual measures are performed.

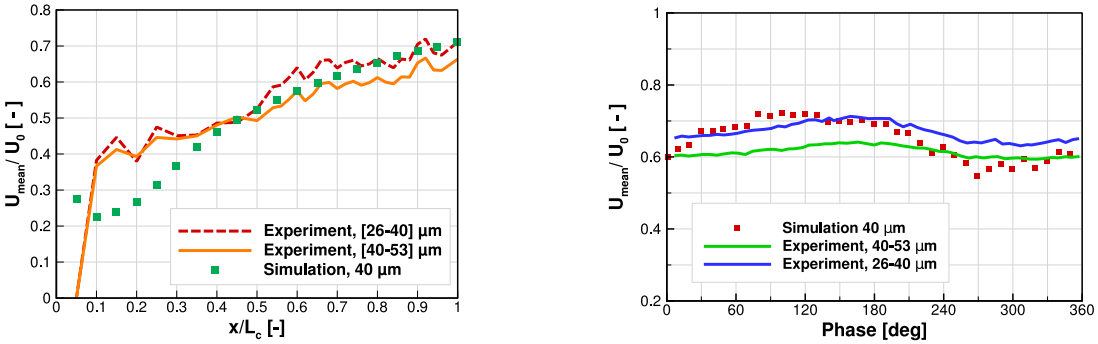

(a) Average particle stream-wise velocity

(b) Particles phase delay at $x/L_C = 0.8$

Figure 7. Droplets behaviour in the duct: (a) average velocity; (b) phase averaged velocity and delay.

Film behaviour

Droplet impingement was observed on both the upper and the lower walls. The upper wall is subject to the impact of the droplets leaving the main liquid body at the considered operating point[4]. **Figure 8(a)** shows the upper wall film thickness profiles in the span-wise direction, at different abscissae. This film is therefore formed by the impact of the droplets generated from the column breakup (only a small fraction of the droplets generated from the stripping mechanism were found impacting, mainly the lower wall). **Figure 8(b)** presents the longitudinal profile of the upper wall film at the last simulation time-step. Three full oscillation periods were simulated: three main waves are therefore visible in both the thickness and velocity plots. These are directly linked to the higher liquid deposition in the low gas velocity phase, see **Figure 4(e-f)**. The film main features are therefore visibly affected by the acoustic perturbation. However, at the moment no validation data are available for the film behaviour. First experimental observations would suggest a film of *~200-400 µm* on the upper wall, quite comparable with the numerical values.

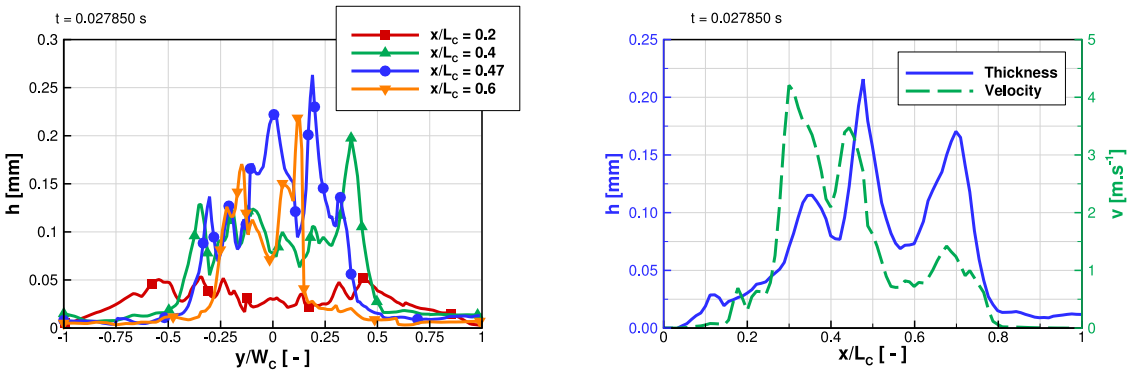

(a) Instantaneous span-wise (x = const.) profile

(b) Instantaneous thickness and velocity profiles on the centreline (y = 0).

Figure 8. Liquid film profiles on the upper wall of the duct. (a) Span-wise (*x = const.*) profiles for several abscissae. (b) Thickness and instantaneous velocity on the centreline (*y = 0*).

Conclusion

This paper presented a multi-solver unsteady numerical approach for the simulation of atomization in presence of acoustic perturbations, as may be encountered during the development of combustion instabilities. This approach was tested against the ONERA SIGMA test rig experience (Bodoc, Desclaux et al.[4]), which is representative of a single injection point of a multi-point aeronautical injector. A LJICF atomizes in a confined duct, subject to an imposed planar acoustic wave generated by a loudspeaker; the acoustic fluctuating velocity induces a periodical flapping motion of the liquid column, leading to a periodical fluctuation of the spray density and velocity. Wall droplet impinging is modulated by the acoustic forcing as well.

The multi-solver approach of the ONERA CEDRE code was used with three key ingredients:

[4] Too much large *q* values (i.e. larger liquid injection velocities) make the liquid jet to directly impact the wall (Thuillet [15]), a configuration for which the dispersed phase/film approach is no longer adapted.

- a multi-fluid approach for the liquid column simulation and an atomization model to generate the spray;
- a Lagrangian dispersed-phase approach for the spray evolution;
- a Shallow-Water film solver to deal with particles impinging the walls.

The CEDRE simulation was compared to the experimental results of the SIGMA experience. The perturbed simulation showed a noticeable response from the jet behaviour and the consequent droplet formation, as the jet oscillated at the imposed frequency. The simulated liquid column trajectories were evaluated by phase averaging, and were found to match the experimental results. The spray of droplets was created as soon as the multi-fluid solution was found under-resolved. A fixed droplet diameter was imposed, no predictive model being currently available. The droplet behaviour was again investigated by global and phase averaging. The results showed good agreement in the second half of the duct, where the correct average velocity and phase delay were found. However, larger deviations were found in the proximity of the jet, near the atomization zone. A more accurate investigation of the droplet initial characteristics should therefore be carried out. A thin liquid film was observed, in particular on the upper wall, its presence being confirmed by experimental visualizations on the test rig. The liquid film presented waves directly correlated to the oscillations of the jet and the more important impinging rates in the lower velocity phases.

The proposed numerical method has shown a promising potential to improve industrial LES simulations of fuel injection by taking in account atomization unsteady effects in the spray formation, as well as interactions with film forming at the walls.

Acknowledgements

The financial support of the Direction Générale de l'Armement (DGA), the French Government Defense procurement and technology agency, is gratefully acknowledged.

References

[1] J. Apeloig. Étude expérimentale du rôle de la phase liquide dans les phénomènes d'instabilités thermoacoustiques agissant au sein de turbomachines diphasiques. Ph.D. thesis, ONERA (2013)

[2] M. Bauerheim, G. Staffelbach, N. Worth, J. Dawson, L. Gicquel, et al.. Sensitivity of LES-based harmonic flame response model for turbulent swirled flames and impact on the stability of azimuthal modes. Proceedings of the Combustion Institute, Elsevier, 35(3), 3355-3363 (2015) <10.1016/j.proci.2014.07.021>, <hal-01116162>

[3] G. Blanchard, D. Zuzio, P. Villedieu. A large scale multi-fluid/dispersed phase approach for spray generation in aeronautical fuel injectors. ICMF 2016, Florence, Italy (2016) hal-01441814

[4] V. Bodoc, A. Desclaux, P. Gajan, Frank Simon, G. Illac. Characterization of confined liquid jet injected into oscillating air crossflow. INCA Colloquium, Saclay (2017)

[5] S. Candel, D. Durox, T. Schuller, P. Palies, J.-F. Bourgouin, J. P. Moeck. Progress and Challenges in Swirling Flame Dynamics. Comptes Rendus Mecanique, 340 (11–12), 758–768 (2012)

[6] CEDRE, Manuel theorique. CEDRE website: http://www.cedre.onera.fr

[7] S. Ducruix, T. Schuller, D. Durox, S. Candel. Combustion dynamics and instabilities: elementary coupling and driving mechanisms. Journal of Propulsion and Power, 19(5), 722-734 (2003)

[8] P. Gaillard, C. Le Touze, L. Matuszewski, A. Murrone. Numerical Simulation of Cryogenic Injection in Rocket Engine Combustion Chambers, Challenges in Combustion for Aerospace Propulsion (2016) <10.12762/2016.AL11.16>, <hal-01369627>

[9] C. Laurent, Modeling of drop reemission on a small scale rotating fan model: comparison between experimental and numerical results, 7th European Conference for Aeronautics and Space Sciences EUCASS, Milan (2017)

[10] F. Nicoud, T. Poinsot. Thermoacoustic Instabilities: Should the Rayleigh Criterion be Extended to Include Entropy Changes?, Combustion and Flame, 142(1–2), 153–159 (2005) <doi:10.1016/j.combustflame.2005.02.013>

[11] T. Poinsot, Prediction and control of combustion instabilities in real engines. Proceedings of the Combustion Institute, 36(1), 1-28, ISSN 1540-7489 (2017)

[12] A. Refloch, B. Courbet, A. Murrone, P. Villedieu, C. Laurent, P. Gilbank, J. Troyes, L. Tessé, G. Chaineray, J.B. Dargaud, E. Quémerais, F. Vuillot, CEDRE Software, Aerospace Lab Journal, http://www.aerospacelab-journal.org/CEDRE-Software

[13] K. A. Sallam, C. Aalburg, G. M. Faeth. Breakup of round nonturbulent liquid jets in gaseous crossflow. AIAA Journal, 42(12), 2529-2540 (2004)

[14] S. Thuillet, Multiscale simulation of the atomization of a liquid jet in oscillating gaseous cross-flow, PhD Thesis ONERA-ISAE, https://hal.archives-ouvertes.fr/tel-02023561/document, (2018)

[15] P. K. Wu, K. A. Kirkendall, R. P. Fuller, A. S. Nejad. Breakup processes of liquid jets in subsonic crossflows. Journal of Propulsion and Power, 13(1), 64-73 (1997)